Influence of Titanium Tetrabutoxide on Nanoindentation and Nanoscratch Profiles of Silsesquioxane Films

Lijiang Hu, Di Wang, Zushun Lu, Yanwei Song, Changmei Song*

Summary: Based on silsesquioxanes (SSO) derived from the hydrolytic condensation of [3-(glacildoxy)propyl]trimethoxysilane (GPMS), 20 wt-% tetraethoxysilane (TEOS) and titanium tetrabutoxide (TTB), two-layer SSO films were prepared for nanoindentation and nanoscratch tests. The tests were carried out to study the influence of different amounts of TTB in the two-layer hybrid films on hardness (*H*), elastic modulus (*E*) and scratch (*S*) testing profiles. The *H* profiles of the modified films showed two kinds of *H* corresponding to the two–layer structure. In the *S* testing profiles, all final–scan profiles did not absolutely coincide or overlap with the first–scan profiles. All *S* profiles revealed a fluctuanting characteristic and all *S* profiles can be divided into two regions in the horizontal displacement, because of the two-layer structure. The film containing an adequate amount of TTB (20 wt-%) was found to possess the largest *H* and *E*, as well as the best *S* resistance.

Keywords: elastic modulus; film; hardness; nanoindentation; nanoscratch; scratch; silsesquioxane; titanium tetrabutoxide

Introduction

Similar types of organically modified silicates are based on the hydrolytic condensation of a titanium tetrabutoxide with a trialkoxysilane having an organic moiety with a polymerizable group (epoxy, vinyl, etc.).[1] In these hybrid materials, two different types of networks may be formed: 1) an organic network produced by the cross-linking of the polymerizable groups, and 2) an inorganic network based on Si–O–Si and Ti–O–Ti bonds. The fraction of a titanium tetrabutoxide in the initial formulation will determine the prevalent network in the final structure and the resulting mechanical properties of the hybrid materials. These organically modified silicates have received much attention recently because of their applications, such as optical waveguides, corrosion resistance.[2,3] These hybrid materials suffer from phase segregation to generate a two–layer structure.[4,5] The upper layer is based on $EtSiO_{1.5}$ and the lower layer is based on TiO_2. The photocatalytic decomposition of surface organic groups on a TiO_2 lower layer has been previously reported.[6,7]

In this paper, the focus is on the effect of modifier contents on nanoindentation and nanoscratch performances for the silsesquioxane films modified with the titanium tetrabutoxide. The aim is to determine how the profiles are influenced by the fabricated two–layer structure and whether the hardness, elastic modulus and scratch resistance (or abrasion) could be improved by varying the amount of additional titanium tetrabutoxide.

Experimental Part

For sol preparation, first, [3–(glacidoxy)-propyl]trimethoxysilane (GPMS) and titanium tetrabutoxide (TTB) were pre-hydrolyzed separately: GPMS with a modifier of 20 wt-% tetraethoxysilane (TEOS) in ethanol was

Department of Applied Chemistry, Harbin Institute of Technology, Box 713, Harbin 150001, China
E-mail: hulijiang@vip.sina.com

hydrolyzed with formic acid in a 0.5:1 molar ratio with respect to Si for 5 days at 40 °C; the TTB in the ethanol was hydrolyzed with hydrochloric acid in a 0.05:1 molar ratio with respect to Ti for 4 days at 40 °C and then for 10 days at 70 °C. The mole ratios of ethanol and H_2O with respect to both Si and Ti were 4 and 3, respectively. Nest GPMS and 5, 10, 15, 20 and 25 wt-% TTB were placed in beakers, respectively, and then stirred continuously for 5 hours at 35 °C. The silsesquioxane (SSO) modified with TEOS and TTB will be denoted as GTST (GPMS–TEOS–SSO–TTB).

For coatings on glass substrates, first, the resulting GTST was diluted with ethanol in a weight ratio of 1:30 and then ethylenediamine (EDA) was added into the solution. The EDA added to the diluted SSO was determined as the amount which gave the maximum glass transition temperature (119 °C) of the cured product.[8] Next dip–coating was performed on glass substrates (76.4 mm × 25.2 mm × 1.2 mm) at 270 mm/min. Finally the coated glasses were cured in an oven for 6 hours at 80 °C and then for 2 hours at 120 °C and 135 °C, respectively. GTST films with different TTB will be denoted as f–GTST$_{i\%}$ ($i = 5, 10, 15, 20$ and 25).

The thickness of the f–GTST (1.4 μm) was determined using a Hitachi S–570 scanning electron microscope (SEM) device.

H and *E* of the coating systems were determined using a Nano Indenter XP® (MTS Systems Corporation) device. A triangular pyramid Berkovich indenter was used to fabricate the tip radius. Its indent shape and side view angles were 65.3° and 12.95°, respectively. The Poisson ratio (0.3) of the hybrid coatings was estimated as $\nu = 0.225$. Due to the fact that it enters as $(1-\nu^2)$ in the calculation of *E*, an error in the estimation of the Poisson ratio does not produce a significant effect on the resulting value of the elastic modulus.[9] Using the set of experimental curves obtained for every type of coating, average values of *H* and *E* as a function of displacement were generated, together with the corresponding standard deviations. Both the harmonic frame stiffness and the frame stiffness correction were 0 Nm^{-1}. Loading was controlled such that the loading rate divided by the load was held constant at 0.05 s^{-1}, and the unloading in stiffness calculation was 50%. Tests were performed in a clean–air environment with a relative humidity of approximately 30%, while the temperature was kept constant at 23 ± 0.5 °C.[10]

Scratch testing was measured using a NanoIndenter XP® system with options for lateral–force measurements. The procedure was similar to that presented in detail elsewhere.[11] Before scratching, an initial surface profile of the samples was detected by pre–scanning the surface with the indenter under a low load of 100 μN. Depths of scratches with increasing scratch length were measured *in–situ* by profiling the surface of the film before, during and after the scratch test, resulting in a total length (pre-scan track) of 700 μm for the test while the scratch length (scratch scan) was 600 μm as applied to all f–MST$_{i\%}$. The test was repeated several times for each system. The normal indenter load was linearly ramped from the minimum to the maximum (0–5 mN) during the scratching. The translation speed was typically 50 μm s^{-1}.[12]

Results and Discussion

For a soft-film/hard-substrate coating system, *H* and *E* profiles of the film can be divided into four regions (or layers):[13] 1) the superficial region; 2) the region of maximum value and the pile–up effect; 3) the plateau region of a constant value where the intrinsic *H* and *E* of the coating may be determined (see Table 1); and 4) the region showing a substrate effect. The local values of *H* and *E* of f–GTST$_{i\%}$ as a function of penetration are shown in Figure 1a and 1b. The influence of the different TTB contents in the films on the *H* and *E* is clearly observed. The *H* profile of f–GTST$_{i\%}$ as shown in Figure 1a is different from one in a normal soft-film/hard-substrate coating system.[13] There are two sets of the four-region profile, showing the two kinds of intrinsic H_1 and H_2 in the limited

Table 1.
Nanoindentation and nanoscratch data of the f–GTST coatings.

TTB/wt%	f–GTST$_{5\text{-}25\%}$			Scratch first-ramp region		Highest scratch depth/nm	Highest residual depth/nm
	H_1/GPa	H_2/GPa	E/GPa	starting/nm	ending/nm		
5	0.37 ± 0.01 (51–93 nm)[a)]	1.01 ± 0.01 (323–389 nm)	4.61 ± 0.01 (37–42 nm)	97	155 (−469)[b)]	−1147	−315 (596)[c)]
10	0.47 ± 0.01 (52–93 nm)	1.21 ± 0.02 (282–343 nm)	6.92 ± 0.06 (25–37 nm)	106	166 (−503)	−974	−511 (575)
15	0.59 ± 0.01 (67–93 nm)	1.29 ± 0.02 (323–413 nm)	7.24 ± 0.05 (31–44 nm)	102	150 (−434)	−849	−473 (594)
20	0.62 ± 0.02 (51–93 nm)	1.21 ± 0.02 (215–322 nm)	9.49 ± 0.27 (19–31 nm)	105	1((−393)	−807	−487 (524)
25	0.59 ± 0.01 (54–93 nm)	1.24 ± 0.02 (264–322 nm)	8.68 ± 0.27 (19–31 nm)	107	167 (−456)	−843	−581 (567)
30	–	–	–	106	151 (−381)	−834	−487 (575)

[a)]Depth regions for determining intrinsic H and E values. [b), c)]Scratch depth corresponding to the ending displacement.

range of 51–93 nm and 323–389 nm, respectively, which can be compared to a two-layer microstructure of f–GTST$_{i\%}$ where the upper layer consists mainly of epoxy-SSO-SiO_2 and the lower layer consists mainly of TiO_2.[1] The two-layer microstructure was generated because there is a different self-condensation ratio between n(epoxy-SSO-SiO_2) and $n$$TiO_2$ which grow individually even when mixed together. Figure 1b shows the similar four-region profiles but a fluctuation occurs in a region of about 200–400 nm depending on the TTB content, providing evidence of the two-layer structure even the E value is difficult to measured.

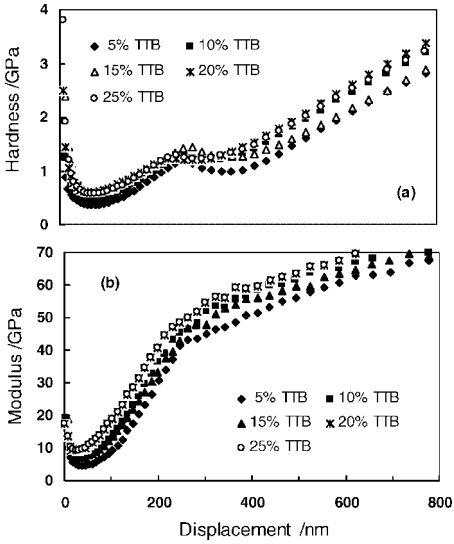

Figure 1.
Influence of different TTB contents on (a) hardness and (b) elastic modulus of the f–GTST$_{i\%}$ (i = 5, 10, 15, 20 and 25).

The H_1 and E values increase with an increase in the TTB content from 5 to 20 wt-% fraction. The values decrease after a content of 20 wt-% TTB when additional TTB was added, leading to a looser structure in f-GTST$_{25\%}$. F–GTST$_{20\%}$ has the maximum average H_1 (0.62 GPa) and E (9.49 GPa) measured in the third region, respectively.

The two-layer structure of f-GTST$_{i\%}$ shows similar nanoscratch profiles for all six profiles as shown in Figure 2a–f. 1) All final–scan profiles do not absolutely coincide or overlap with the first–scan profiles; all residual depth (difference between the pre and post–scan profiles) regions[14] show poor recovery behaviour and poor elasto–plastic deformation of the films; 2) all S profiles reveal a fluctuating characteristic; and 3) all S profiles can be divided into two–ramp regions in the horizontal displacement, which can be attributed to the two-layer structure. However, there are still some differences among the six profiles.

For f–GTST$_{5\%}$ (see Figure 2a), the S tip can easily penetrate the surface layer during the S ramping and can result in the highest vertical displacement of about 1147 nm, implying poorer H or S resistance. This

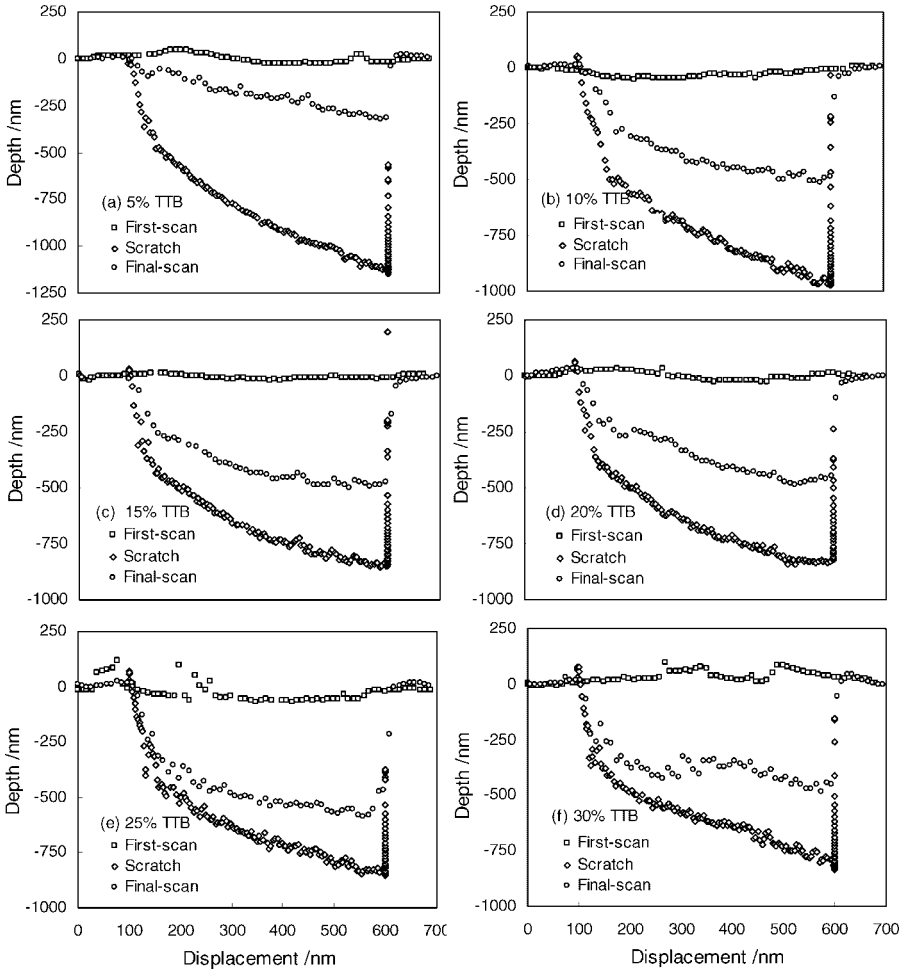

Figure 2.
Influence of the different TTB contents on the *S* profiles. (a) 5, (b) 10, (c) 15, (d) 20, (e) 25 and (f) 30.

procedure also results in a large friction force at the beginning of the *S* and in an increase in the coefficient of friction from 0 to 0.59 under a loading 0–0.31 mN (see Figure 3). The residual depth is obviously shorter due to a small addition of TTB which maintains the viscoelasticity of the epoxy–SSO film. For f–GTST$_{10\%}$, the *S* tip can easily penetrate the surface layer as well. The fluctuating scratch profile of f–GTST$_{10\%}$ in the first–ramp region (106–166 nm) descends sharply to a depth of 503 nm due to the soft upper layer. After the ending displacement of the first–ramp region, the components of SSO–SiO_2–TiO_2 and TiO_2

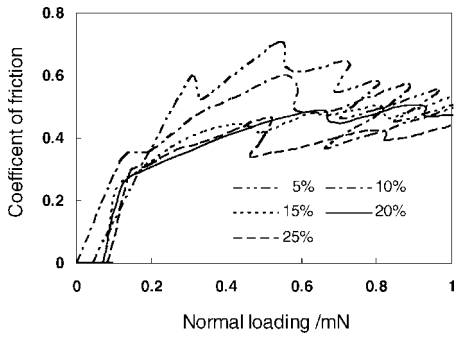

Figure 3.
Friction coefficient of f–GTST$_{i\%}$ ($i = 5, 10, 15, 20$ and 25) as a function of *S* load.

become richer, the film hardens and the *S* profile is barred from a sharp decline. The final–scan profile does not absolutely overlap with the first–scan profile and does not depend exclusively on plasticity and hardness but is related to the adhesive strength between the film and the substrate.[15] Perhaps the fluctuating profiles indicate that the film was partially delaminated by ploughing or was peeled off during *S* testing.[11,16]

The *S* and final–scan profiles of f–GTST$_{15\%}$ and f–GTST$_{20\%}$ are better and shallower than the *S* and final-scan profiles of f–GTST$_{10\%}$ (see Figure 2c and 2d), indicating better layer structures and mechanical properties (*H*, *E* and *S* resistance) due to an adequate fraction of TTB in the films and the formation of the desirable microstructure. For both films, there are very few seriously abrupt changes in the *S* and the final–scan profiles, implying that the films did not peel off during *S* ramping.[11] Figure 3 shows the lowest friction coefficient for f–GTST$_{20\%}$ (0.36 under a loading of 0–0.31 mN).

F–GTST$_{25\%}$ and f–GTST$_{30\%}$ demonstrate seriously fluctuating profiles due to the addition of more TTB.[10] The generated SSO–SiO_2–TiO_2 or TiO_2 in the lower layer may decrease the adhesive strength between the film and the substrate by decreasing in the connection of Si atoms on the substrate surface, making the films easy to peel off and to become seriously damaged during *S* ramping, resulting in abrupt changes in the *S* and the final–scan profiles.[16]

Conclusions

Based on SSO modified with different amounts of TTB, two–layer f–GTST$_{i\%}$ was prepared for nanoindentation and nanoscratch tests. The *H* profile of f-GTST$_{5\text{-}25\%}$ showed two obvious kinds of H_1 and H_2 corresponding to the two–layer structure. The H_1 and *E* values increased with an increase in the TTB content from 5 to 20 wt-% fraction and the values decreased after a content of 20 wt-% TTB due to more additions of TTB. In the *S*–testing profiles of f-GTST$_{i\%}$, all final–scan profiles did not absolutely coincide or overlap with the first–scan profiles, all *S* profiles revealed a fluctuanting characteristic and all *S* profiles can be divided into two–ramp regions in the horizontal displacement, because of the two-layer structure. For f–GTST$_{20\%}$, the H_1 (0.62 GPa) and *E* (9.49 GPa) were relatively large. Better *S* resistance and stronger adhesion shown in the *S*–testing profiles were ascribed to adequate amounts of TTB in the modified f–GTST$_{20\%}$ which enhances abrasion or *S* resistance of the film and makes it suitable as protective coatings.

Acknowledgements: The financial supports (GB04A204 and ZJG0506-02) from Department of Science and Technology of the Government of Heilongjiang Province, are grateful acknowledged.

[1] A. Matsuda, T. Sasaki, K. Tadanaga, M. Tatsumisago, T. Minami, *Chem. Mater.* **2002**, *14*, 2693.
[2] W. Que, Y. Zhou, Y. L. Lam, Y. C. Chan, C. H. Kam, *Appl. Phys. A* **2001**, *73*, 171.
[3] T. L. Metroke, O. Kachurina, E. T. Knobbe, *Prog. Org. Coat.* **2002**, *44*, 295.
[4] D. C. M. Dutoit, M. Schneider, A. Baiker, *J. Catal.* **1995**, *153*, 165.
[5] K. Tadanaga, J. Morinaga, A. Matsuda, T. Minami, *Chem. Mater.* **2000**, *12*, 590.
[6] H. Tada, *Langmuir* **1996**, *12*, 966.
[7] H. Tada, M. Tanaka, *Langmuir* **1997**, *13*, 360.
[8] R. Ruseckaite, L. Hu, C. C. Riccardi, R. J. J. Williams, *Polym. Inter.* **1993**, *30*, 287.
[9] L. Hu, X. Zhang, Y. Sun, R. J. J. Williams, *J. Sol–Gel Sci. Tech.* **2005**, *37*(1), 41.
[10] L. Hu, X. Zhang, Y. Huang, *Plast. Rub. Comp.* **2004**, *33*(9), 457.
[11] C. Charitidis, Y. Panayiotatos, S. Logothetidis, *Diam. Relat. Mater.* **2003**, *12*, 1088.
[12] X. Zhang, L. Hu, D. Sun, *Acta Mater.* **2006**, *54*, 5469.
[13] L. Hu, X. Zhang, H. You, Y. Liu, H. Zhang, D. Sun, *J. Mater. Sci.* **2004**, *39*, 1331.
[14] P. Lemoine, J. F. Zhao, J. P. Quinn, A. A. Ogwu, J. A. McLaughlin, P. Maguire, F. McGinnity, X. Shi, *Wear* **2000**, *244*, 79.
[15] J. M. Sanchez, S. E. Mansy, B. Sun, T. Scherban, N. Fang, D. Pantuso, W. Ford, M. R. Elizalde, J. M. M. Esnaola, A. M. Meizoso, J. G. Sevillano, M. Fuentes, J. Maiz, *Acta Mater.* **1999**, *47*, 4405.
[16] L. Huang, K. Xu, J. Lu, *Diam. Relat. Mater.* **2001**, *10*, 1448.

